Food Chemistry 498 (2026) 147134

Contents lists available at ScienceDirect

Food Chemistry

journal homepage: www.elsevier.com/locate/foodchem

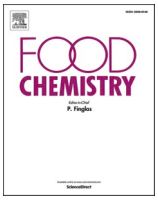

Ultrasound-assisted extraction of water-soluble components from olive stones: Chemical characterization and functionalities

Francesca Trevisiol [a], Niccolò Renoldi [a,*], Asja Brovedani [a], Alfredo Rondinella [b], Marilena Marino [a], Clara Comuzzi [a], Amina Maalej [c], Mohamed Chamkha [c], Hana Maalej [d], Nadia Innocente [a], Maria Cristina Nicoli [a], Sonia Calligaris [a]

[a] Department of Agri-Food, Environmental and Animal Sciences, University of Udine, Udine, Italy
[b] Polytechnic Department of Engineering and Architecture, University of Udine, Udine, Italy
[c] Laboratory of Environmental Bioprocesses, Centre of Biotechnology of Sfax, P.O. Box 1177, 3018 Sfax, Tunisia
[d] University of Gabes, Faculty of Sciences of Gabes, Laboratory of Biodiversity and Valorization of Arid Areas Bioresources (BVBAA), LR16ES36, Faculty of Sciences, Erriadh 6072, Gabes, Tunisia

ARTICLE INFO

Keywords:
Ultrasound-assisted extraction
Olive stones
Bioactive compounds
By-products valorization
Antimicrobial activity
Emulsion

ABSTRACT

This study explores the potential of ultrasonication as an efficient and sustainable technology to improve the extraction of water-soluble components from olive stones (OS), a by-product of the olive industry. OS were milled into powder (OSP), and aqueous suspensions were treated with ultrasound for increasing times. The resulting aqueous extracts (US-AE) were analyzed for chemical, physicochemical, and functional properties. Increasing ultrasonication time enhanced the phenolic content (from 247.5 ± 1.0 to 367.3 ± 0.7 mg GAE/g_{dw}) and promoted the release of high-molecular-weight (> 100,001 Da) compounds (from 7.05 ± 0.49 to 11.82 ± 0.11 %) derived from the disruption of the lignocellulosic material. US-AE exhibited remarkable antioxidant activity (DPPH, FRAP), antimicrobial capacity against pathogens and spoilage microorganisms, and the ability to produce stable emulsions for up to 30 days, while exhibiting no cytotoxicity. This research demonstrated the feasibility of ultrasonication in obtaining novel ingredients from OS, within a circular economy framework.

1. Introduction

The production of olive oil represents a crucial economic sector, particularly in Mediterranean countries, where olives have historically been a key agricultural product. The growing awareness of olive oil's health benefits has driven a threefold increase in global production over the past 60 years, reaching over 3 million tons by 2020–2021 (IOC, 2022). Although the olive sector provides significant economic benefits and health advantages, it also faces considerable environmental challenges due to the substantial waste generated during the whole production chain (Manzanares et al., 2020). In the European Union alone, the olive oil industry generates an estimated 21.4 million tons of by-products each year (Donner et al., 2022). This includes approximately 11.8 million tons from the pruning of olive trees and around 9.6 million tons per year from olive mills, which consist of by-products such as olive pomace, mill wastewater, and olive stones (OS) (Berbel & Posadillo, 2018). The limited industrial applications for these wastes, coupled with the seasonality of olive oil production that generates large quantities of waste in a short period, result in high management and disposal costs (Enaime et al., 2024; Nunes et al., 2016). These by-products should be considered economic resources; however, the potential applications of OS are still largely underexplored, despite their contribution of approximately 18–25 % to the total weight of olive fruit (Montegiove et al., 2024; Nunes et al., 2016). This leads to an estimated global annual production ranging from 4.1 to 5 million tons (Bai et al., 2023; Rodríguez et al., 2008). As lignocellulosic biomass, OS primarily consist of cellulose (27.1–36.4 %), hemicellulose (24.5–32.2 %), and lignin (23.1–40.4 %) intimately associated (Mallamaci et al., 2021; Sánchez-Borrego et al., 2021). The proportion of these components can vary depending on the olive variety and cultivation conditions (Christoforou & Fokaides, 2016). Lignocellulosic residues can also contain additional components, such as pectin, proteins, and various extractives, including tannins, lipids, resins, steroids, terpenes, terpenoids, flavonoids, and phenolic compounds, in proportions that depend on the biomass source

* Corresponding author at: Department of Agricultural, Food, Environmental and Animal Sciences, University of Udine, Via Sondrio 2/A, 33100 Udine, Italy.
E-mail address: niccolo.renoldi@uniud.it (N. Renoldi).

https://doi.org/10.1016/j.foodchem.2025.147134
Received 23 July 2025; Received in revised form 10 November 2025; Accepted 14 November 2025
Available online 17 November 2025

(Mujtaba et al., 2023). Many of these compounds can exhibit biological activities, including antioxidant and antimicrobial (Gomes-Araújo et al., 2021). Moreover, surface-active molecules with potential in emulsion stabilization can also be extracted, as demonstrated by Mikkonen (2020) and Valoppi, Lahtinen, et al. (2019); Valoppi, Maina, et al. (2019). Currently, OS are primarily utilized as biofuel for combustion, converting biomass into thermal energy and power (Gomez-Martin et al., 2018). Minor applications of OS include their biochemical conversion into bioethanol, as well as the production of biosorbent materials (Cuevas et al., 2021; Serafin et al., 2023). Other proposed applications include high-fibre animal feed supplements, plastic fillers, and cosmetic products (Carraro et al., 2005; Ferreiro-Cabello et al., 2022; Rodríguez et al., 2008; Siracusa et al., 2001).

On the other hand, the literature on possible food applications of OS remains very limited. While some studies have explored the inclusion of OS-derived ingredients in food products like biscuits, sponge cake, bread, yoghurt, and tea, their wider application and comprehensive effects on food properties are still largely unexplored (Bolek, 2020; Cakir et al., 2023; Jahanbakhshi & Ansari, 2020; Oncel & Ozbek, 2025).

The tight association of cellulose, hemicellulose, and lignin in the lignocellulosic biomass that constitutes OS limits its use in food products. This complex structure provides strong mechanical and chemical resistance, hindering access to its components for recovery and valorization (Chen et al., 2024). A potential solution is to extract the target compounds through pre-treatments. Conventional pretreatments require high temperatures, substantial amounts of water and chemical reagents, prolonged extraction times, and low yields, often associated with component degradation and high processing costs (Anukam & Berghel, 2020). Conventional pre-treatment methods have been applied to lignocellulosic materials from various sources, including wheat bran, oil palm trunks, sugarcane bagasse, and OS (Nair et al., 2017; Noparat et al., 2015; Peng et al., 2009; Saleh et al., 2014). Non-conventional methods, such as microwaves, supercritical fluids, high hydrostatic pressure, and ultrasound (US), provide alternatives to conventional ones, aiming to improve extractability while minimizing environmental impacts by reducing solvent use and energy consumption (Martinez-Solano et al., 2021; Sidana & Yadav, 2022). Among these methods, US-assisted extraction is a promising technology for valorizing lignocellulosic biomasses (Martinez-Solano et al., 2021; Wang, Tallian, et al., 2018). This method relies on acoustic cavitation, where the collapse and implosion of gas microbubbles create localized high-energy zones that disrupt lignocellulosic fibers, reducing their length, increasing the accessibility for chemical and enzymatic reactions, and enhancing release of target compounds (Kumar et al., 2023; Wang, Tallian, et al., 2018). Studies on bamboo fibre and corn cobs report higher yields and purity of extracted hemicellulose and phenolic compounds using US compared to conventional methods (Wang, Tallian, et al., 2018; Yang et al., 2009). Additionally, US treatment can modify polysaccharide structures, affecting techno-functional properties such as swelling, water-holding capacity, oil-holding capacity, as well as enhancing antioxidant activity, thermal, and rheological properties (Jambrak et al., 2010;Kaur & Gill, 2019; Wu et al., 2022). These effects are likely caused by chain fragmentation and distortion of crystalline regions of polysaccharides induced by cavitational forces (Kaur & Gill, 2019; Wu et al., 2022). These changes enhance the usability of lignocellulosic biomasses and introduce new valuable attributes for the food industry (Martinez-Solano et al., 2021). US-assisted techniques have been widely applied to olive oil processing residues, including pomace, pruning materials, and leaf biomass, for the recovery of bioactive compounds (Gómez-Cruz et al., 2021; Gullón et al., 2018). However, to our knowledge, their application to OS remains largely unexplored in the current literature.

Based on these considerations, this study investigated the feasibility of ultrasound technology as a green and innovative approach to enhance the extractability of water-soluble compounds from the lignocellulosic matrix of olive stones. To this aim, 5 % (*w*/w) aqueous suspensions of olive stone powder were treated with US for increasing times. After ultrasonication, the aqueous extracts were separated from the insoluble residue and characterized for their chemical and physicochemical properties. Furthermore, antioxidant and antimicrobial activities, as well as cytotoxicity, were determined to elucidate their biological functionalities. Finally, since potentially surface-active molecules could be extracted, the emulsifying capacity of the extracts was also tested. These findings unlock novel pathways for the valorization and upscaling of olive stone biomass in a circular economy framework.

2. Materials and methods

2.1. Preparation of olive stones powder (OSP)

OS, recovered as a by-product from the extraction of extra virgin olive oil from a blend of olive cultivars, were kindly supplied by the Consortium of Extra Virgin Olive Oil Producers of Friuli Venezia Giulia (Udine, Italy). The olives were harvested between October and November 2023. The stones were collected directly at the production site, sealed in plastic bags, and stored under vacuum at −18 °C until further processing. OS were thawed at room temperature for 2 h and dried in an oven (UM100, Memmert, Schwabach, Germany) at 40 °C for 2 h, resulting in a moisture content of 9.80 ± 0.14 %. Grinding was carried out using a ball mill (MM 500 VARIO, Retsch, Haan, Germany) operating at 25 Hz for 2 min. The resulting powder (OSP) was sieved (Digital Electromagnetic Sieve Shaker, Filtra Vibrácio, Barcelona, Spain) to isolate particles smaller than 0.5 mm.

2.2. Preparation of the ultrasound-aqueous extracts (US-AE)

The extracts were prepared following the method of Freitas et al. (2022) with modifications. Aliquots of 500 mL of 5 % (*w*/w) OSP suspensions prepared in Milli-Q water were stirred overnight at room temperature. The suspensions were then placed in 600 mL beakers with external cooling jackets connected to a cryostat (PC200 Immersion Circulators, Thermo Fisher Scientific, Milan, Italy) set to −5 °C. The system was provided with an US titanium probe with a diameter of 22 mm (UP400S, Hieschler Ultrasonics GmbH, Teltow, Germany), centrally inserted into the suspension. Samples were treated at a frequency of 24 kHz for 30, 60, and 120 min, with a maximum sample temperature of 15 °C. The treated suspension was then centrifuged (Avanti Centrifuge™ J-25, BeckMan, Milan, Italy) at 20,000 ×*g* for 20 min at 20 °C and filtered using filter paper (Whatman No. 1) in a Büchner funnel to recover the aqueous extract (US-AE, respectively labelled US-AE30, US-AE60, US-AE120). The US-AE0 sample, which was not subjected to US treatment, served as the control sample. A portion of the US-AE was freeze-dried (Laboratory and Pilot Freeze-Dryer Mini-Fast Edwards, Model 1700, Edwards High Vacuum, Milan, Italy), while the remaining part was utilized in its liquid form. Samples were stored in a freezer at −18 °C until further analysis. Each US treatment was performed at least twice on separate days ($n = 2$).

2.3. Physicochemical and chemical characterization of the US-AE

2.3.1. Dry matter

The dry matter (DM) of the US-AE was determined using a gravimetric method on 2 g of sample, measuring the weight change before and after overnight drying in a vacuum oven (Vuotomatic 50, Bicasa, Milan, Italy) at 75 °C. The dry matter was calculated using the following equation:

$$\mathrm{DM}\ (\%) = \frac{H - S}{S} \times 100 \quad (1)$$

where S is the weight of the sample before drying (g), and H is the weight of the sample after drying (g).

Table 1
Dry matter content (mg/g), pH, and molecular weight distribution (%) of the US-assisted aqueous extracts (US-AE) sonicated for 0, 30, 60 and 120 min, respectively named US-AE0, US-AE30, US-AE60, US-AE120.

		US-AE0	US-AE30	US-AE60	US-AE120
Dry matter		0.51 ± 0.01[b]	0.64 ± 0.01[a]	0.65 ± 0.03[a]	0.69 ± 0.02[a]
pH		7.14 ± 0.01[a]	6.58 ± 0.01[d]	6.67 ± 0.01[b]	6.62 ± 0.01[c]
Molecular weight (Da) distribution (%)					
	106 < x < 50,000	52.47 ± 0.93[a]	46.51 ± 0.67[b]	44.79 ± 1.10[b]	46.87 ± 0.87[b]
	50,001 < x < 100,000	41.09 ± 0.36[a]	44.87 ± 1.08[a]	43.46 ± 2.07[a]	41.37 ± 0.58[a]
	x > 100,001	7.05 ± 0.49[b]	9.04 ± 0.96[b]	11.42 ± 0.13[a]	11.82 ± 0.11[a]

Different letters mean statistically different values within the same row ($p < 0.05$).

Table 2
HPLC determination of free sugars (mg/mL) and total phenolic content (TPC, mg GAE/g_{dw}) of the US-assisted aqueous extracts (US-AE) sonicated for 0, 30, 60 and 120 min, respectively named US-AE0, US-AE30, US-AE60, US-AE120.

	US-AE0	US-AE30	US-AE60	US-AE120
Glucose	1.28 ± 0.01[a]	1.04 ± 0.01[c]	1.14 ± 0.01[b]	1.12 ± 0.02[b]
Mannitol	1.30 ± 0.01[a]	0.99 ± 0.01[b]	1.12 ± 0.01[ab]	0.98 ± 0.10[b]
TPC	247.5 ± 1.0[d]	276.2 ± 1.7[c]	310.9 ± 0.8[b]	367.3 ± 0.7[a]

Different letters mean statistically different values within the same row ($p < 0.05$).

2.4. pH

The pH of US-AE was measured using a pH meter (pH 301, HANNA Instruments, Padua, Italy) previously calibrated with standard solutions at pH 4, 7, and 9. Measurements were directly performed by immersing the electrode in the US-AE after allowing the sample to return to room temperature after the US treatment.

2.4.1. Determination of molecular weights

Samples were prepared by dissolving 22 mg of freeze-dried US-AE in 1.5 mL of distilled water and filtered using a 0.45 μm nylon membrane before injection. The molecular mass was determined by size exclusion high-performance liquid chromatography (SEC-HPLC). The LC-4000 HPLC system (Jasco Europe, Cremella, Italy) equipped with 20 μL sample loop and a refractive index detector RI-4030 module (Jasco Europe, Cremella, Italy) was used. The separation was carried out by combining a PL Aquagel-OH 50 column (8 μm, 300 × 7.5 mm, Agilent Technologies, Santa Clara, CA, USA) with a PL Aquagel-OH 30 column (8 μm, 300 × 7.5 mm, Agilent Technologies, Santa Clara, CA, USA). Analysis was performed in isocratic mode at a 1 mL/min flow rate with distilled water as mobile phase and the column oven set at 25 °C, while the RI set at 40 °C. A calibration curve obtained with standards of polyethylene glycol/polyethylene oxide (PEG/PEO) of different molecular weights (range 100–500.000 g/mol, InfinityLab EasiVial, Agilent Technologies, Santa Clara, CA, USA) was used to estimate the US-AE molecular weight.

2.4.2. Scanning electron microscopy (SEM)

The microstructure of freeze-dried US-AE was observed via a field-emission scanning electron microscopy (FE-SEM, JEOL JSM7610F+, Tokyo, Japan). Samples were mounted on specimen holders with copper tape and coated with gold using a Sputter Coater 108 auto (Cressington Scientific Instruments Ltd., Watford, UK). Images of the samples were obtained in secondary electron mode at 5 kV and two magnifications (250× and 1000×).

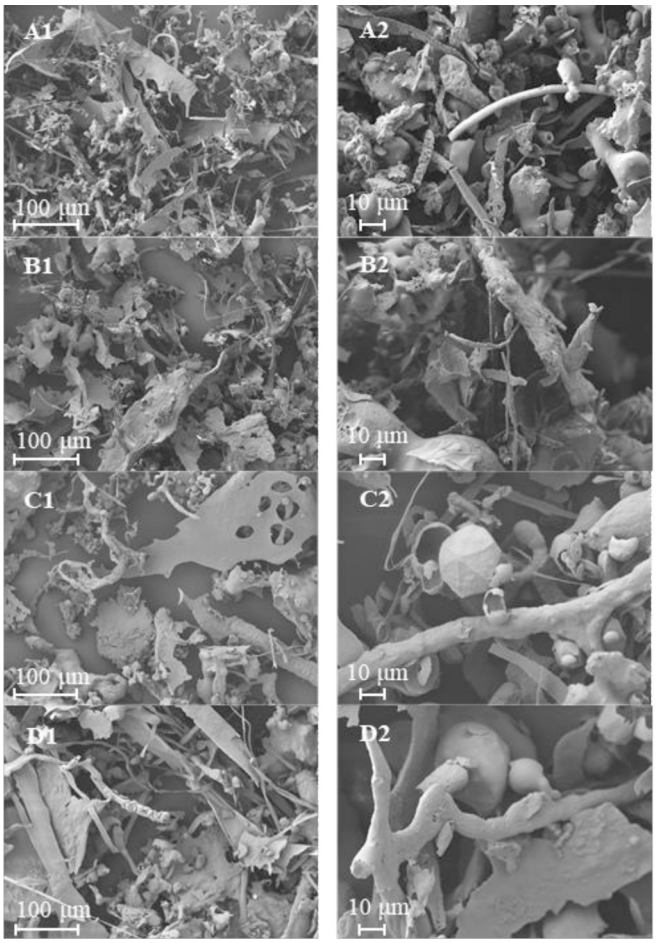

Fig. 1. Scanning electron microscopy images of the aqueous extracts sonicated for 0, 30, 60 and 120 min, respectively named US-AE0 (A), US-AE30 (B), US-AE60 (C), and US-AE120 (D). Magnifications of 250× (A1-D1) and 1000× (A2-D2).

2.4.3. Nuclear magnetic resonance (NMR)

Samples for NMR analysis were prepared by dissolving 5 mg of each freeze-dried US-AE in D_2O (0.6 mL; Sigma-Aldrich, Missouri, USA); the ^1H spectra were acquired at 25 °C by a Bruker Avance III 400 MHz digital NMR spectrometer (Bruker, Karlsruhe, Germany). The Bruker noesygppr1d sequence was used to acquire 1D ^1H spectra suppressing the solvent. DSS was used as an external standard for ^1H reference. Spectra were recorded using Bruker pulse sequences. For identification, mannitol and glucose standards (Sigma Aldrich, St. Louis, Missouri, USA) were used.

2.4.4. Determination of free sugars

For the determination of free sugars, 10 mg of freeze-dried US-AE were solubilized in 1 mL of distilled water. Samples were stirred for 2 h and then filtered using 0.45 μm PVDF syringe filters. Separation and quantification of free sugars were carried out using a LC-4000 HPLC system equipped with an Aminex HPX-87H ion exclusion column (300 mm × 7.8 mm × 9 μm; BioRad, Hercules, CA), a 20 μL sample loop, and an oven set at 50 °C. Isocratic elution was performed at 0.6 mL/min with 5 mM H_2SO_4 as mobile phase. Sugars were detected using the RI-4030 module. Data analysis was performed using the ChromNav software (Jasco Europe, Cremella, Italy) and the amount of glucose and mannitol was determined by external calibration ($R^2 = 0.99$) with standard

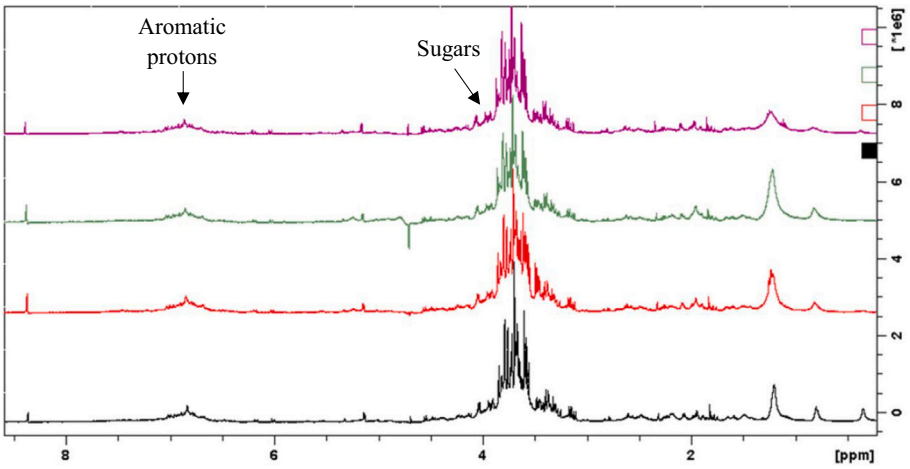

Fig. 2. ^{1}H NMR spectra of the aqueous extracts sonicated for 0, 30, 60 and 120 min, respectively named US-AE0 (black), US-AE30 (red), US-AE60 (green) and US-AE120 (purple). (For interpretation of the references to colour in this figure legend, the reader is referred to the web version of this article.)

solutions at different concentrations (0.1–3.0 mg/mL).

2.4.5. Total phenolic content (TPC)

Total polyphenolic content was determined using the Folin-Ciocalteau reagent (Singleton & Rossi, 1965). The reaction mixture consisted of 250 µL of US-AE, 18.5 mL of distilled water, 1250 µL of Folin-Ciocalteau reagent (Sigma Aldrich, Milan, Italy), and 5 mL of a sodium carbonate solution (0.15 g/mL). Following a 2-h reaction at ambient temperature, the absorbance of the mixture was measured at 750 nm using a spectrophotometer (UV-2501PC, Shimadzu Corporation, Kyoto, Japan). A calibration curve was obtained using a standard solution of gallic acid at different concentrations ($R^2 = 0.99$). The results were expressed as milligrams of gallic acid (Sigma Aldrich, Milan, Italy) equivalents (GAE) per gram of dry matter of US-AE.

2.4.6. Identification and quantification of polyphenolic compounds

Chromatographic analysis was carried out following the method described by Maalej et al. (2017). The analyses were performed using an Agilent 1260 series HPLC-DAD system (Agilent, Waldbronn, Germany). Compound separation was achieved on a ZORBAX Eclipse XDB-C18 column (4.6 mm internal diameter, 250 mm length, 3.5 µm particle size). The mobile phase consisted of two solvents: phase A (0.1 % acetic acid in water) and phase B (100 % acetonitrile).

Before analysis, freeze-dried US-AE were dissolved in ultra-pure water. A gradient elution program was applied at a flow rate of 0.5 mL/min, with a sample injection volume of 5 µL, and the column temperature was maintained at 40 °C. The gradient profile was as follows:

- 0–22 min: 10–50 % B.
- 22–32 min: 50–100 % B.
- 32–40 min: 100 % B.
- 40–44 min: 100–10 % B.

A re-equilibration phase of 6 min was applied between runs. Detection was performed using a diode array detector (DAD), scanning wavelengths from 190 to 400 nm, with primary detection at 254, 280, and 330 nm. Identification of compounds was based on UV absorption spectra, retention times, and mass spectra obtained using an ion trap mass detector (MSD Trap XCT). Quantification was performed using a four-point calibration curve ($R^2 = 0.99$) with authentic external standards whenever available. Results were expressed as milligrams of each identified compound per gram dry matter of US-AE.

2.5. Biological functionalities of the US-AE

2.5.1. Antioxidant activity

2.5.1.1. 2,2-Diphenyl-1-picrylhydrazyl (DPPH) radical scavenging assay. The DPPH radical scavenging ability was determined following the method of Brand-Williams et al. (1995). Briefly, 120 µL of a methanolic DPPH solution (0.1 mg/mL) (Sigma Aldrich, Milan Italy) were mixed with 80 µL of US-AE. After 40 min of incubation at 25 °C in the dark, absorbance was measured at 517 nm (Sunrise, Tecan, Milan, Italy). Results were expressed as mg Trolox (Sigma Aldrich, Milan Italy) equivalents (TE) per g of dry matter of the US-AE using a standard curve prepared from Trolox standard solutions ($R^2 = 0.99$).

2.5.1.2. Ferric reducing antioxidant power (FRAP) assay. The FRAP assay was determined following the method of Benzie and Strain (1996) with few modifications. The FRAP reagent was prepared by mixing acetate buffer (pH 3.6), 10 mM 2,4,6-Tris(2-pyridyl)-1,3,5-triazine (TPTZ) (Sigma Aldrich, Milan, Italy) in 40 mM HCl, and 20 mM $FeCl_3$ (Sigma Aldrich, Milan, Italy) in a 10:1:1 ratio. For each sample, 100 µL of US-AE and 100 µL of FRAP reagent were combined, and absorbance was recorded at 593 nm after 50 min at 37 °C. Results were expressed as mg of Trolox equivalents (TE) per g of dry matter using a calibration curve prepared from Trolox standard solutions ($R^2 = 0.99$).

2.5.2. Antimicrobial activity

The antimicrobial activity of freeze-dried US-AE was tested against *Listeria monocytogenes* Scott A, *Salmonella enterica* subsp. *arizonae* DSM9386, *Staphylococcus aureus* DIAL317, *Escherichia coli* DIAL4315 and *Pseudomonas fluorescens* DIAL22 (Innocente et al., 2019). The strains were stored at −80 °C in Brain Heart Infusion Broth (BHI; Oxoid, Milan, Italy) with added glycerol (Sigma Aldrich, Milan, Italy) at 30 % *v*/v. Before each test, one loopful of each culture was used to inoculate 1 mL of BHI broth and incubated at 37 °C for 18 h. Each culture was centrifuged at 13,000 xg for 5 min in a Mirko 20 centrifuge (Hettich S.r.l., Milan, Italy), washed 3 times with Maximum Recovery Diluent (MRD; Oxoid, Milan, Italy), and diluted in MRD at a ratio of 1:100,000.

Antimicrobial activity was evaluated by a turbidimetric method in 96-well U-bottom polystyrene microplates (Corning Incorporated, New York, USA). Duplicate wells contained 200 µL of BHI with added US-AE (5 and 10 mg/mL) and 10 µL of microbial culture. Control wells (CTRL) containing BHI were inoculated with the target microorganisms, and white wells containing only BHI were also prepared. The microplates were incubated at 37 °C for 48 h in a Sunrise microplate reader (Tecan, Cernusco s. N., Milan, Italy), and the optical density at 630 nm was read

Table 3
HPLC quantification (mg/g_{dw}) of identified phenolic compounds and ascorbic acid of the US-assisted aqueous extracts (US-AE) sonicated for 0, 30, 60 and 120 min, respectively named US-AE0, US-AE30, US-AE60, US-AE120.

Compound	Retention time (min)	Quantity			
		US-AE0	US-AE30	US-AE60	US-AE120
Ascorbic acid	4.34	0.00 ± 0.00^{a}	0.54 ± 0.02^{b}	7.08 ± 0.31^{c}	7.03 ± 0.09^{c}
Gallic acid	7.20	0.07 ± 0.01^{b}	0.82 ± 0.03^{c}	0.07 ± 0.01^{b}	0.01 ± 0.00^{a}
3,4-Dihydroxybenzoic acid	10.46	0.05 ± 0.01^{c}	0.01 ± 0.00^{a}	0.02 ± 0.00^{b}	0.05 ± 0.01^{c}
Caffeic acid	13.43	0.26 ± 0.01^{a}	0.33 ± 0.03^{bc}	0.35 ± 0.03^{c}	0.28 ± 0.01^{ab}
Epicatechin	13.80	1.41 ± 0.05^{b}	1.45 ± 0.06 ^{b}	1.52 ± 0.08 ^{b}	1.14 ± 0.01^{a}
Vanillic acid	14.19	0.06 ± 0.00^{a}	0.12 ± 0.01^{b}	0.17 ± 0.02^{c}	0.14 ± 0.01^{b}
Rutin	15.21	0.32 ± 0.02^{b}	0.32 ± 0.03^{b}	0.37 ± 0.02^{b}	0.26 ± 0.01^{a}
Verbascoside	15.93	0.66 ± 0.03^{ab}	0.71 ± 0.05^{b}	0.93 ± 0.07^{c}	0.57 ± 0.02^{a}
Luteoline glucoside	16.28	0.15 ± 0.01^{b}	0.80 ± 0.02^{d}	0.32 ± 0.01^{c}	0.11 ± 0.01^{a}
p-Coumaric acid	17.01	0.02 ± 0.00^{a}	0.14 ± 0.01^{c}	0.05 ± 0.00^{b}	0.05 ± 0.00^{b}
Ferulic acid	18.25	1.29 ± 0.05^{d}	0.56 ± 0.05^{c}	0.15 ± 0.02^{a}	0.34 ± 0.01^{b}
Apigenin-7-glucoside	18.28	0.44 ± 0.03^{a}	0.64 ± 0.02^{b}	1.00 ± 0.03^{c}	0.50 ± 0.04^{a}
Cinnamic acid	18.93	0.42 ± 0.03^{c}	0.46 ± 0.04^{c}	0.31 ± 0.02^{b}	0.05 ± 0.01^{a}
Naringenin	21.04	4.34 ± 0.07^{a}	5.65 ± 0.08^{b}	6.16 ± 0.14^{c}	4.46 ± 0.09^{a}
Luteolin	22.65	0.20 ± 0.01^{b}	0.20 ± 0.03^{b}	0.05 ± 0.00^{a}	0.25 ± 0.05^{b}
Quercetin	23.23	0.16 ± 0.01^{a}	0.38 ± 0.02^{b}	0.16 ± 0.02^{a}	0.13 ± 0.02^{a}
Apigenin	25.67	0.06 ± 0.00^{a}	0.10 ± 0.01^{b}	0.09 ± 0.01^{b}	0.11 ± 0.02^{b}

Different letters mean statistically different values within the same row ($p < 0.05$).

at 30 min intervals (Bisson et al., 2023). OD_{630} readings were used to generate turbidimetric curves. The data were modeled using the Baranyi model (Baranyi & Roberts, 1994) (Eq. 2) implemented within the Excel add-in DMFit to obtain the lag phase length (λ, expressed in h), the maximum growth rate (μ_{max}, expressed in OD/h), and the maximum optical density (OD_{max}, expressed in OD):

$$OD(t) = OD_0 + \left(OD_{max} - OD_0\right) \times \frac{e^{\mu maxA(t)} - 1}{e^{\mu maxA(t)} - 1 + e^{\mu max\lambda}} \quad (2)$$

2.5.3. Cytotoxicity assessment

Human embryonic Kidney (HEK-293) Cells and Hepatocellular carcinoma (HepG2) cells viability was analyzed by measuring the conversion of MTT into the purple formazan, a property distinctive of cells with active metabolism. Cells were seeded in 96-well plates at a density of 3×10^4 cells/well and incubated overnight in a CO_2 incubator at 37 °C. The plates were treated with freeze-dried US-AE at different concentrations (25–1600 μg/mL) for 48 h. The medium was then removed, 100 mL new medium and 10 mL MTT solution (5 mg/mL) were added and incubated at 37 °C for 4 h. Finally, 100 mL SDS (10 %) was used to dissolve the formazan crystals. The optical density was measured at 570 nm using a microplate reader (Thermo Scientific Varioskan Flash) (Maalej et al., 2017).

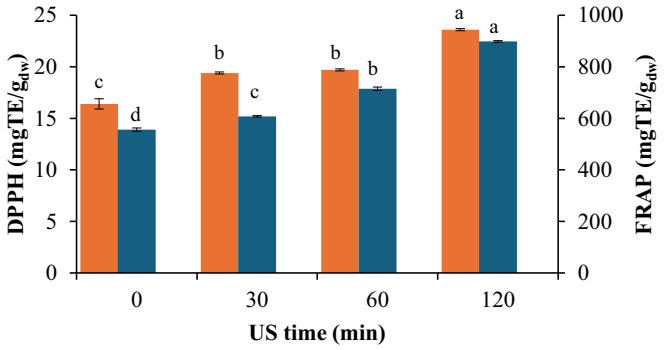

Fig. 3. DPPH (blue) and FRAP (orange) the US-assisted aqueous extracts (US-AE) sonicated for 0, 30, 60 and 120 min, respectively named US-AE0, US-AE30, US-AE60, US-AE120. Different letters mean statistically different values within the same assay ($p < 0.05$). (For interpretation of the references to colour in this figure legend, the reader is referred to the web version of this article.)

2.6. Emulsifying properties

Each US-AE was used to prepare emulsions following the method described by Melchior et al. (2022) with a few modifications. Sunflower oil was added to the US-AE at two concentrations (0.5 % and 1.0 % *w/w*), and the mixtures were pre-homogenized using a high-speed mixer (Polytron PT3000, Littau, Switzerland) at 10,000 ×g for 3 min. Samples were then treated using a continuous lab-scale high-pressure homogenizer (Panda Plus 2000, GEA Niro Soavi, Parma, Italy) at 150 MPa. After homogenization, 0.02 % (*w/v*) sodium azide (Sigma Aldrich, Italy) was added to prevent microbial growth during storage at 20 °C for up to 30 days. The resulting emulsions were placed in 10 mL glass vials, and then, 10 μL of the sample was pipetted from the bottom and diluted to 2 mL with 0.1 % SDS solution at 0 and 120 min after homogenization. The absorbance values related to the emulsifying activity index (EAI) and the emulsifying stability index (ESI) at 120 min were measured using spectrophotometry at 500 nm. These indices were calculated as described by Melchior et al. (2022) using the following equations:

$$\mathrm{EAI}\left(\mathrm{m}^2 g_{dw}^{-1}\right) = \frac{2 \times 2.303 \times A_0 \times \mathrm{DF}}{C \times (1-\theta) \times \Phi \times 10000} \quad (3)$$

$$\mathrm{ESI\ (min)} = \frac{A_0}{A_0 - A_{120}} \times 120 \quad (4)$$

where DF is the dilution factor (200), C is the initial concentration of US-AE, θ is the oil fraction in the emulsion, Φ is the optical path length (1 cm), and A_0 and A_{120} are the absorbance values of the emulsion at 0 and 120 min, respectively.

2.6.1. Size distribution analysis and ζ-potential

Particle size distribution and ζ-potential of emulsions were measured at 25 °C using a dynamic light scattering (DLS) system (NanoSizer 3000, Malvern Instruments, Malvern, UK). The refractive index and viscosity were estimated to match those of pure water at 25 °C, recorded as 1.33 and 0.890 mPa·s, respectively. Particle size was expressed as the

Table 4
Kinetic parameters and model fit parameters obtained from turbidimetric curves obtained in the presence of the US-assisted aqueous extracts (US-AE) sonicated for 0, 30, 60 and 120 min, respectively named US-AE0, US-AE30, US-AE60, US-AE120.

Target	Sample	λ (h)	μ_{max} (OD/h)	OD_{max}	SE	R^2
L. monocytogenes	CTRL	6.00 ± 0.09[a]	0.16 ± 0.01[a]	1.19 ± 0.09[a]	0.04	0.99
	US-AE0	6.04 ± 0.02[a]	0.06 ± 0.00[b]	0.57 ± 0.03[c]	0.00	0.99
	US-AE30	2.60 ± 0.57[b]	0.05 ± 0.01[b]	0.88 ± 0.11[b]	0.04	0.98
	US-AE60	2.05 ± 0.38[b]	0.05 ± 0.00[b]	0.95 ± 0.08[ab]	0.04	0.98
	US-AE120	3.28 ± 0.11[b]	0.06 ± 0.00[b]	0.94 ± 0.01[ab]	0.05	0.98
Salm. enterica subs. *Arizonae*	CTRL	3.39 ± 0.07[a]	0.28 ± 0.01[a]	1.35 ± 0.00[a]	0.08	0.98
	US-AE0	3.58 ± 0.16[a]	0.17 ± 0.01[b]	1.08 ± 0.00[c]	0.01	0.99
	US-AE30	3.20 ± 0.43[a]	0.17 ± 0.03[b]	1.08 ± 0.02[c]	0.06	0.98
	US-AE60	3.62 ± 0.00[a]	0.18 ± 0.00[b]	1.14 ± 0.00[b]	0.05	0.99
	US-AE120	3.25 ± 0.01[a]	0.17 ± 0.01[b]	1.12 ± 0.01[b]	0.06	0.98
Staph. aureus	CTRL	4.07 ± 0.04[b]	0.56 ± 0.06[a]	1.36 ± 0.01[a]	0.04	1.00
	US-AE0	4.83 ± 0.09[a]	0.24 ± 0.00[b]	1.01 ± 0.14[b]	0.03	1.00
	US-AE30	5.14 ± 0.13[a]	0.21 ± 0.01[b]	1.13 ± 0.04[ab]	0.03	1.00
	US-AE60	4.76 ± 0.16[a]	0.25 ± 0.02[b]	1.12 ± 0.04[ab]	0.04	0.99
	US-AE120	4.93 ± 0.10[a]	0.27 ± 0.03[b]	1.18 ± 0.04[ab]	0.04	0.99
E. coli	CTRL	3.12 ± 0.09[a]	0.50 ± 0.01[a]	1.44 ± 0.01[a]	0.08	0.98
	US-AE0	3.13 ± 0.02[a]	0.33 ± 0.00[bc]	1.20 ± 0.07[b]	0.00	0.98
	US-AE30	2.89 ± 0.05[b]	0.30 ± 0.02[c]	1.27 ± 0.01[b]	0.08	0.98
	US-AE60	3.10 ± 0.01[a]	0.37 ± 0.03[b]	1.25 ± 0.01[b]	0.07	0.98
	US-AE120	2.87 ± 0.04[b]	0.32 ± 0.01[bc]	1.28 ± 0.01[b]	0.07	0.98
P. fluorescens	CTRL	9.85 ± 0.11[a]	0.14 ± 0.00[a]	0.80 ± 0.11[a]	0.02	1.00
	US-AE0	8.92 ± 0.70[ab]	0.06 ± 0.00[b]	0.45 ± 0.03[b]	0.01	1.00
	US-AE30	8.87 ± 0.00[ab]	0.07 ± 0.00[b]	0.45 ± 0.00[b]	0.01	1.00
	US-AE60	8.27 ± 0.19[b]	0.05 ± 0.00[b]	0.49 ± 0.02[b]	0.01	1.00
	US-AE120	8.76 ± 0.15[ab]	0.06 ± 0.01[b]	0.47 ± 0.03[b]	0.01	1.00

For each microorganism, means in the same column followed by different letters are statistically different ($p < 0.05$); SE, standard error of fit; R^2, coefficient of determination.

intensity-weighted average diameter in nm.

2.6.2. Image acquisition

Images of emulsions were obtained using an image acquisition cabinet (Immagini & Computer, Bareggio, Italy) equipped with a digital camera (EOS 550D, Canon, Milan, Italy). The images were saved in JPEG format with a resolution of 3456 × 2304 pixels. For emulsions, images were captured for up to 30 days to monitor stability over time.

2.7. Data analysis

The results are presented as the mean ± standard deviation, calculated from two replicate experiments ($n = 2$), with each experiment representing the average of at least three analytical measurements. Bartlett's test was performed to assess the homogeneity of variances across all data groups. Statistically significant differences between group means were evaluated using one-way analysis of variance (ANOVA), followed by Tukey's HSD test, with significance set at $p < 0.05$ with OriginPro 9.0 software (OriginLab Corporation, Northampton, Massachusetts, USA). For microbial growth modeling, the standard error of fit (SE) and coefficient of determination (R^2) were estimated using the online tool DMFit, available at the Combase website (https://combase.errc.ars.usda.gov/).

3. Results and discussion

3.1. Physicochemical and chemical characterization of the US-AE

Dry matter, pH, and molecular weight distribution of the AE-US obtained at different extraction times (0, 30, 60 and 120 min) are presented in Table 1.

The data show an increase in dry matter, with values for US-AE30, US-AE60, and US-AE120 significantly higher than those of US-AE0. This suggests that US treatment may favour the solubilization of water-soluble compounds, such as compounds with acid moieties, able to lower the pH of the medium (Table 1) compared to non-sonicated samples (US-AE0). This indicates that US treatment may favour the solubilization of water-soluble compounds, possibly including acidic components, which could contribute to the observed decrease in pH in the sonicated samples compared to the non-sonicated sample (Table 1). These findings align with previous research studies, which indicated that US treatment led to a pH decrease in plant-based matrices due to the release of organic acids from cellular structures (Jambrak et al., 2007).

The extract obtained without US treatment (US-AE0) was predominantly composed of low molecular weight compounds (106–50,000 Da), suggesting that water extraction alone primarily solubilized small and readily extractable molecules, such as sugars (Table 2). In contrast, increasing the duration of US-assisted extraction promoted the release of higher molecular weight fractions. Specifically, US-AE60 and US-AE120 exhibited a marked increase in the proportion of compounds exceeding 100,000 Da, possibly associated with the destructuring of the lignocellulosic material. It should be noted that OS are primarily composed of insoluble fibre (around 90 %), consisting of cellulose and hemicellulose, tightly embedded with lignin (Rodríguez et al., 2008).

These findings are further supported by the increase in dry matter content observed in the US-treated extracts (Table 1), indicating that US enhanced the extraction of otherwise inaccessible macromolecular structures, due to the mechanical disruption of the lignocellulosic material. Similar results were reported by Hromádková et al. (1999), who enhanced the extractability of polysaccharides from *Salvia officinalis* through US-assisted extraction, demonstrating a significant improvement in yield compared to conventional extraction.

Microstructure of US-AE was investigated using scanning electron microscopy (Fig. 1A-D.)

It can be noted that morphological changes occurred as a consequence of the US-assisted water extraction process. Fig. 1A shows the structural changes due to the aqueous extraction without US, which resulted in the release of a variety of compounds, some with lamellar structures, others tubular, and some globular, highlighting the complexity of the extracted matrix. Prolonged US treatments caused a progressive disruption of the lignocellulosic matrix, allowing the release of increasingly larger compounds that were otherwise trapped within the biomass structure (Fig. 1B-D). These observations were consistent with the HPLC-SEC results (Table 1).

^{1}H NMR was performed to better understand the composition of the US-AE, and the spectra are presented in Fig. 2.

Several strongly overlapping signals attributable to aromatic protons are visible in the spectral region between 6.75 and 7.20 ppm. The aromatic signals may be associated with both polyphenols naturally found

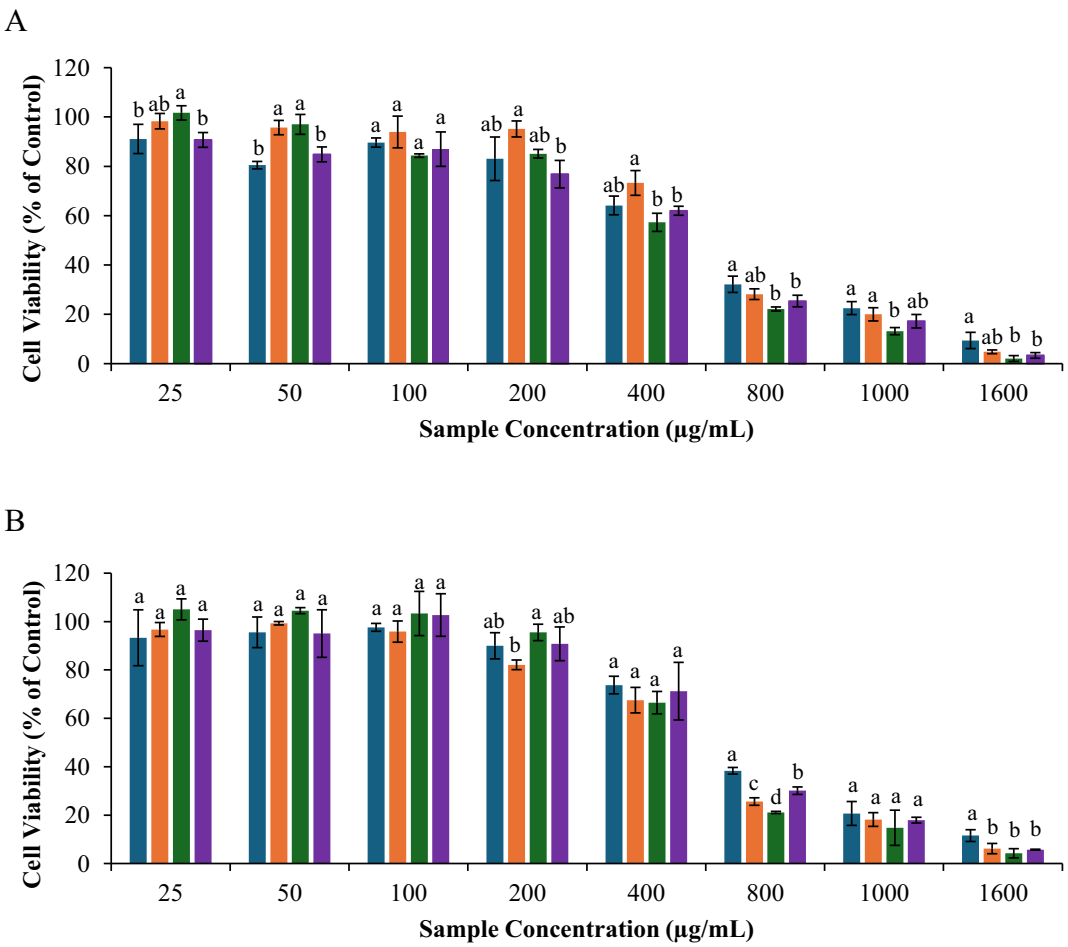

Fig. 4. Cell viability of HEK-293 (human embryonic kidney) (A) and HepG2 (human hepatocellular carcinoma) (B) cells treated with the US-assisted aqueous extracts (US-AE) sonicated for 0, 30, 60 and 120 min, respectively named US-AE0 (blue), US-AE30 (orange), US-AE60 (green), US-AE120 (purple) at different concentrations for 48 h. Different letters indicate statistically significant differences ($p < 0.05$) between treatments. (For interpretation of the references to colour in this figure legend, the reader is referred to the web version of this article.)

Table 5
Physicochemical properties of emulsions produced with the US-assisted aqueous extracts (US-AE) sonicated for 0, 30, 60 and 120 min, respectively named US-AE0, US-AE30, US-AE60, US-AE120.

Oil (%w/w)		EAI (m^2/g_{dw})	ESI (min)	ζ-potential (mV)	Particle size distribution			
					PDI	Peak 1 (nm)	Peak 2 (nm)	Peak 3 (nm)
0.5 %	US-AE0	143.7 ± 0.6^{a}	482.0 ± 8.5^{d}	-40.1 ± 0.1^{c}	0.38 ± 0.0^{a}	182.3 ± 13.9^{a}	579.9 ± 5.6^{a}	4805 ± 90.5^{a}
	US-AE30	140.0 ± 4.2^{ab}	2551.5 ± 6.4^{a}	-32.1 ± 0.4^{a}	0.25 ± 0.0^{b}	–	365.5 ± 3.2^{b}	4956 ± 21.2^{a}
	US-AE60	134.0 ± 1.4^{b}	1442.0 ± 8.5^{b}	-32.85 ± 0.1^{a}	0.27 ± 0.0^{b}	–	348.2 ± 5.0^{b}	4948 ± 198.0^{a}
	US-AE120	101.3 ± 0.6^{c}	935.5 ± 5.0^{c}	-38.5 ± 0.1^{b}	0.26 ± 0.3^{b}	–	309.3 ± 3.0^{c}	4703 ± 139.3^{a}
1 %	US-AE0	187.5 ± 5.0^{a}	543.5 ± 6.4^{c}	-24.6 ± 0.7^{b}	0.44 ± 0.0^{a}	110.7 ± 14.7^{a}	459.1 ± 4.0^{a}	4566 ± 93.3^{b}
	US-AE30	127.0 ± 2.8^{b}	997.0 ± 4.2^{a}	-27.3 ± 0.4^{c}	0.26 ± 0.0^{b}	–	432.3 ± 3.9^{ab}	4706 ± 144.2^{a}
	US-AE60	117.7 ± 2.1^{b}	919.0 ± 1.4^{b}	-17.6 ± 0.1^{a}	0.26 ± 0.0^{b}	–	428.15 ± 0.8^{b}	4905 ± 50.9^{a}
	US-AE120	122.0 ± 3.6^{b}	469.5 ± 3.5^{d}	-23.3 ± 0.3^{b}	0.37 ± 0.1^{a}	–	408.0 ± 12.7^{b}	4990 ± 72.8^{a}

Different letters mean statistically different values within the same column ($p < 0.05$).

in olive stones and low molecular weight phenolic compounds derived from lignin during the ultrasound-assisted extraction process.

The ^{1}H NMR spectra displayed the typical complex pattern of sugars, with the signal of the anomeric protons resonating between 4.47 and 5.20 ppm and the non-anomeric signals strongly overlapping between 3.2 and 4.0 ppm. The spectral region in which the anomeric protons resonate is more reliable for the attribution of signals. The comparison of the spectra of the standard glucose with those of the US-AE showed the presence of glucose in monomeric form, both in the α (5.14 ppm) and β configuration (4.55 ppm), in all the samples analyzed.

The signal intensity of the non-anomeric protons was significantly higher than that of the anomeric protons. This suggests that the spectral range between 3 and 4 ppm likely contains signals from compounds other than sugars. Specifically, some observed signals correspond to mannitol, a polyol produced during photosynthesis. Mannitol is an energy reserve for seed and fruit development and provides osmotic protection against water or salt stress (Doménech et al., 2021). The presence of sugar monomers was also confirmed by HPLC analysis, as reported in Table 2. Since the concentration of free sugars slightly changed upon US treatment, it is likely that they were already present in the matrix, thus not deriving from the breakage of the lignocellulosic material.

Also, TPC linearly increased with the increase of sonication time.

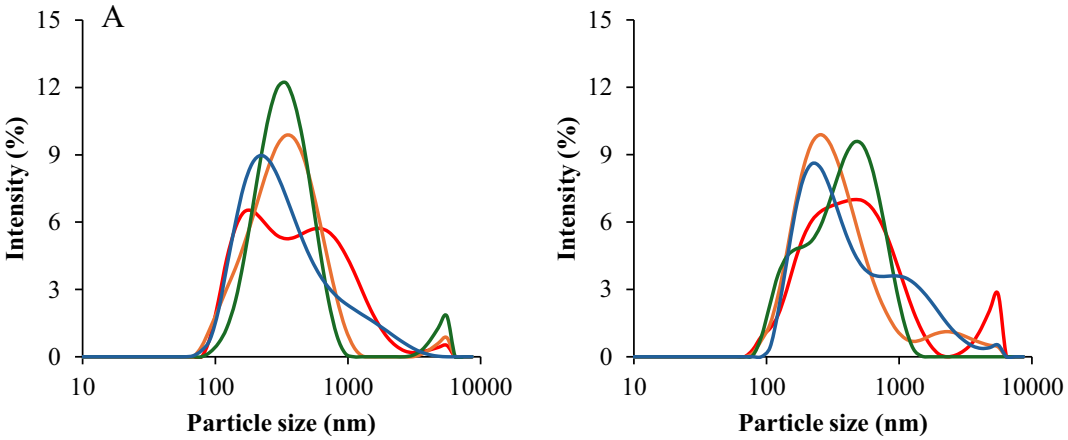

Fig. 5. Particle size distribution of emulsions prepared with the US-assisted aqueous extracts (US-AE) sonicated for 0, 30, 60 and 120 min, respectively named US-AE0 (red), US-AE30 (orange), US-AE60 (grey), US-AE120 (blue). Emulsions with 0.5 % oil (A) and 1 % oil (B). (For interpretation of the references to colour in this figure legend, the reader is referred to the web version of this article.)

Table 6
Stability over time of emulsions prepared with the US-assisted aqueous extracts (US-AE) sonicated for 0. 30. 60 and 120 min. Respectively named US-AE0. US-AE30. US-AE60. US-AE120.

Time (days)	0.5% (w/w) oil				1% (w/w) oil			
	US-AE0	US-AE30	US-AE60	US-AE120	US-AE0	US-AE30	US-AE60	US-AE120
0								
7								
14								
30								

This suggests that US treatment enhanced the phenol yield compared to the untreated aqueous extraction (US-AE0). This result is consistent with studies on other plant-related matrices, such as olive pomace, olive leaves, sugarcane bagasse, and mangosteen hull powder (Cheok et al., 2013; Irakli et al., 2018; Juttuporn et al., 2018; Rodríguez et al., 2022). The extraction of polyphenolic compounds was also confirmed by HPLC analysis (Table 3). The findings highlight significant variations in the phenolic composition of the US-AE as a function of sonication time, confirming that extraction duration plays a crucial role in the release and stability of bioactive compounds. Among the tested conditions, the US-AE60 extract yielded the highest concentration of several bioactive compounds, including naringenin (6.16 mg/g_{dw}), epicatechin (1.52 mg/g_{dw}), verbascoside (0.93 mg/g_{dw}), and apigenin-7-glucoside (1.00 mg/g_{dw}), indicating that 60 min of sonication is optimal for maximizing polyphenol recovery. In contrast, longer sonication (US-AE120) resulted in decreased levels of these compounds, suggesting possible degradation or transformation due to prolonged exposure to acoustic cavitation. Conversely, gallic acid and ferulic acid reached their peak concentrations at US-AE30 (0.82 and 0.56 mg/g_{dw}, respectively), but their levels sharply declined at longer extraction times, which may reflect their higher susceptibility to oxidation or hydrolysis during extended sonication. On the other hand, compounds such as caffeic acid and rutin remained relatively stable across treatments, indicating greater resistance to US-induced structural modifications. These trends are consistent with previous reports highlighting the differential stability of phenolics under US-assisted extraction conditions (Martínez-Patiño et al., 2019; Setyaningsih et al., 2016). Similarly, Jaapar et al. (2017) reported that the longest sonication time (60 min) led to the lowest

concentration and recovery of 6-gingerol, confirming its gradual degradation for prolonged US treatment. Overall, these findings underscore the effectiveness of US-assisted extraction as a green and efficient strategy for recovering phenolic compounds from olive stones, while emphasizing the need to optimize sonication parameters to prevent degradation of sensitive molecules. The increased release of phenolic compounds with ultrasound time likely resulted from lignocellulosic disruption, especially lignin fragmentation, which could release these compounds (Wang, Tallian, et al., 2018). These observations also align well with the results of Gómez-Cruz et al. (2021), who reported similar patterns during polyphenol extraction from olive pomace using US techniques.

3.2. Biological functionalities of the US-AE

Besides the chemical composition, the functionalities of the US-AE were studied. DPPH and FRAP assays were conducted to assess the antioxidant potential of US-AE. Fig. 3 shows the antioxidant activities (DPPH and FRAP) of US-AE at different US extraction times (0, 30, 60 and 120 min).

Both DPPH and FRAP antioxidant activities increased with the US extraction time. Results indicate that the US-AE from OS is highly effective in both reducing ferric ions to ferrous ions and scavenging DPPH free radicals. These properties increased with the sonication time, indicating that US treatment enhances the release of compounds with antioxidant properties from olive stones. The antioxidant activity of US-AE from OS can be associated with the presence of polyphenols and ascorbic acid, but the role of other compounds, such as low molecular weight fibers and mannitol, cannot be excluded (Faraji & Lindsay, 2004). Lo Bianco et al. (2015) reported that olive leaves with higher mannitol content exhibited significantly less oxidative damage under induced oxidative stress, indicating a role for mannitol as a nonenzymatic oxygen radical scavenger in plant tissues.

Moreover, the antimicrobial activity of US-AE was tested against five microbial targets, well-known for their pathogenic and spoilage potential (de Koster & Brul, 2016). US-AE were tested at two concentrations (5 and 10 mg/mL), and in the case of the highest concentration, no growth was observed within 48 h of incubation. On the other hand, at the concentration of 5 mg/mL all microorganisms were able to grow, but their growth was inhibited by US-AE compared to control conditions, as shown in Fig. S1. To quantitatively estimate the inhibitory activity of US-AE, turbidimetric curves were modeled and the kinetic parameters related to the lag phase (λ), exponential phase (μ_{max}), and stationary phase (OD_{max}) of growth were estimated (Table 4).

The presence of US-AE showed to have a growth inhibition effect ($p < 0.05$) on all microbial targets tested, reducing both the maximum growth rate in the exponential phase (μ_{max}) and the maximum OD reached in the stationary phase (OD_{max}). A significant reduction in these kinetic parameters was already observed in the sample sonicated for 30 min, with no proportional improvements at longer extraction times. Regarding the lag phase, *Staph. aureus* was inhibited to some extent, but *Salmonella* did not show inhibition. This phenomenon could be caused by a stimulating effect given by the presence of glucose in US-AE (Table 2), which is metabolized by microorganisms.

The antimicrobial activity of the US-AE under study may be related to the presence of ascorbic acid and phenolic compounds that exhibited broad-spectrum antimicrobial effects by destabilizing bacterial membranes and inhibiting key metabolic enzymes, leading to growth inhibition of Gram-positive and Gram-negative bacteria, including *Salmonella*, *Escherichia*, and *Pseudomonas* species (Lima et al., 2016; Mumtaz et al., 2021). Flavonoids (e.g., quercetin) and their glucosides have demonstrated strong antibacterial effects against *Salmonella* and *Staph. aureus* by damaging the cell wall ultrastructure and cell membrane integrity (Wang, Yao, et al., 2018). In addition, they have been shown to reduce biofilm formation and expression of virulence factors in foodborne pathogens (Kim et al., 2022). The phenolic compound verbascoside, present in significant quantities in aqueous extracts, is also known for its antimicrobial activity, due to the ability to interfere with some membrane-dependent cellular processes (Bazzaz et al., 2018). However, the antimicrobial effect of US-AE does not increase proportionally with the polyphenol content in the samples (Tables 2 and 3) and may also be related to mannitol and other water-soluble compounds released from the lignocellulosic matrix during US treatment (Daglia, 2012; Pace et al., 2019).

To assess the safety profile of the samples, cytotoxicity was evaluated using the MTT assay on HEK-293 and HepG2 cell lines to determine their potential bioactivity and toxicity (Fig. 4).

The cell viability with the addition of 0 μg/mL of sample was 100 % (data not shown). The results revealed a dose-dependent effect, with US-AE30 and US-AE60 maintaining high cell viability (> 80 %) at lower concentrations, suggesting biocompatibility and potential health benefits. In contrast, US-AE120 exhibited increased cytotoxicity, particularly at higher concentrations, likely due to the degradation of phenolics or the formation of oxidative byproducts from prolonged sonication. These findings align with the HPLC analysis, which identified US-AE60 as the optimal extraction condition for maximizing the recovery of bioactive compounds while minimizing degradation. The observed variations between cell lines indicate that HepG2 cells were more sensitive to extraction-induced effects, possibly due to their metabolic activity and response to phenolic compounds (Bartolomei et al., 2021). Overall, the results suggest that US enhances the release of bioactive molecules with promising functional properties, while excessive sonication may compromise extract stability and cellular compatibility. Thus, US-AE60 appears to be the most suitable condition for obtaining bioactive extracts with minimal cytotoxic effects, reinforcing their potential application in functional foods and nutraceutical formulations.

3.3. Emulsifying properties

Table 5 shows emulsifying activity index (EAI), emulsion stability index (ESI), ζ-potential and particle size distribution of emulsions prepared with US-AE used as emulsifiers and oil content at 0.5 % and 1 % *w*/w.

For both oil concentrations, emulsions produced with US-AE0 exhibited the highest EAI values, indicating a greater ability to form an emulsion than those made with sonicated samples. Conversely, the ESI increased with the sonication, reaching a maximum in the US-AE60, likely due to the higher content of phenolic compounds in the extract (Table 3). Valoppi, Lahtinen, et al. (2019) demonstrated that phenolic compounds from softwood extracts can anchor at the water-oil interface, stabilizing emulsions and highlighting their potential as emulsifiers. The ζ-potential provides insights into the surface charge of emulsion particles (Feng et al., 2019). Although there are slight variations between samples (Table 5), ζ-potential values are consistently highly negative in all emulsions, indicating good electrostatic stability. In emulsions with 1 % oil, ζ-potential values are slightly higher, suggesting that the electrostatic stability of emulsions produced with US-AE is influenced more by the oil content than the polyphenolic content. The absolute values of ζ-potential decreased with the extension of US treatment from 60 to 120 min. The reduction in absolute ζ-potential following prolonged ultrasonic treatment is consistent with the observed ESI values, suggesting that this may be due to the formation of aggregates. Fig. 5 shows the particle size distribution of emulsions prepared with US-AE.

All emulsions exhibited a polydisperse particle distribution, as indicated by PDI values exceeding 0.2, and by the particle size distribution profiles showing at least two peaks in all samples, with US-AE0 displaying three peaks and thus the highest heterogeneity (Table 5, Fig. 5) (Melchior et al., 2023). For 0.5 % oil (Table 5, Fig. 5A), the primary particle population of the emulsion containing US-AE0 had a mean size of approximately 580 nm, followed by a smaller population around 180 nm and a larger fraction at around 4800 nm. This sample showed a PDI value of 0.38 that reflects the heterogeneity in particle size

distribution, yet within acceptable limits (Deng et al., 2024). In emulsions with US-AE30, US-AE60, and US-AE120, the primary particle populations were smaller (365, 348, and 309 nm, respectively), with lower PDI values compared to US-AE0. All three samples also exhibited a secondary peak at larger sizes (around 4700–4950 nm), with lower intensity, suggesting the formation of aggregates (Valoppi, Maina, et al., 2019). For 1 % oil (Table 5, Fig. 5B), the emulsion with the US-AE0 sample exhibited a primary particle population of around 459 nm, together with smaller (110 nm) and larger (4560 nm) fractions, confirming its polydispersity, in agreement with the highest PDI value. Emulsions prepared with US-AE30 and US-AE60 showed smaller primary particles (432 and 428 nm, respectively) and lower PDI values, indicating greater uniformity in particle size, although both displayed a secondary peak around 4700–4900 nm, attributable to the formation of some aggregates. The US-AE120 emulsion exhibited the smallest main population (408 nm) but a broader distribution and a similar secondary peak, suggesting possible interaction and aggregation of smaller particles. This result is consistent with Valoppi et al. (2019b), who observed that lignocellulosic emulsifiers may induce particle aggregation. For both oil concentrations, data suggest that particle size decreases with increasing polyphenolic content, which aligns with the findings of Tian et al. (2021) and Xie et al. (2023). They discovered that incorporating polyphenols decreases the oil droplet size, with the magnitude of this reduction modulated by the number of pyrogallol groups in the polyphenol structure. A higher density of these groups facilitates molecular cross-linking, thereby enhancing the stability of the emulsion.

Table 6 presents the stability of emulsions over time, evaluated based on the extent of phase separation. As shown in Table 6, emulsion stability during storage improved with the application of US treatment. Emulsions prepared with US-AE0 exhibited the lowest stability, with phase separation occurring after 7 days. Emulsions produced with US-AE30 and US-AE60 remained stable for 30 days, demonstrating superior long-term stability. In contrast, emulsions produced with US-AE120 showed intermediate stability, with phase separation beginning after 14 days. Emulsions with 1 % oil exhibited more pronounced phase separation compared to those with lower oil content, highlighting the significant influence of oil concentration on emulsion behavior. The enhanced stability of the emulsions prepared with aqueous extracts subjected to US treatment may be attributed to the presence of both polyphenol content and fragments of lignocellulosic material. Tian et al. (2021) observed that the impact of polyphenols on emulsion physical stability was dose-dependent, with lower concentrations enhancing stability, while higher concentrations exhibited the opposite effect. Specifically, the incorporation of relatively high levels of tea polyphenols into emulsions resulted in the formation of small droplets immediately after homogenization; however, these droplets were more prone to aggregation during storage. These findings suggest a pivotal role of polyphenols in influencing emulsion stability over time. Their impact on emulsifying properties appears to depend on the chemical structure and physicochemical characteristics of the phenolic compounds (Di Mattia et al., 2010). The polyphenols in US-AE exhibit the capacity to absorb at the interface, effectively reducing surface tension in a concentration-dependent manner. However, the contribution of other compounds released from the lignocellulosic matrix during sonication cannot be excluded. For instance, Valoppi et al. (2019b) identified wood-derived polysaccharides, specifically galactoglucomannans extracted from spruce, as effective natural emulsifying agents.

4. Conclusions

The results of this study demonstrated the feasibility of using ultrasonication as an efficient treatment to enhance the extraction of water-soluble compounds from olive stones. Specifically, ultrasonication facilitated the disruption of the lignocellulosic matrix, enabling the release of embedded components, primarily polyphenols, as well as the fragmentation of biopolymers. The resulting mixture of compounds endowed the water extracts with notable biological properties, including antioxidant and antimicrobial activities, alongside emulsifying capacity, highlighting their potential for food applications. Importantly, no cytotoxicity was observed for the extracts. These findings outline an innovative strategy for the upcycling of olive stone biomass, emphasizing the potential extracts as novel food ingredients that combine both biological and technological functionalities. Further research is warranted to explore their practical applications in food systems.

CRediT authorship contribution statement

Francesca Trevisiol: Writing – original draft, Methodology, Investigation, Formal analysis. **Niccolò Renoldi:** Writing – review & editing, Visualization, Methodology, Investigation, Data curation. **Asja Brovedani:** Writing – original draft, Formal analysis. **Alfredo Rondinella:** Writing – review & editing, Formal analysis. **Marilena Marino:** Writing – review & editing, Methodology. **Clara Comuzzi:** Writing – review & editing, Methodology, Investigation. **Amina Maalej:** Writing – review & editing, Methodology. **Mohamed Chamkha:** Writing – review & editing, Methodology. **Hana Maalej:** Writing – review & editing, Project administration, Conceptualization. **Nadia Innocente:** Writing – review & editing, Visualization. **Maria Cristina Nicoli:** Writing – review & editing, Conceptualization. **Sonia Calligaris:** Writing – review & editing, Supervision, Funding acquisition, Conceptualization.

Declaration of competing interest

The authors declare that they have no known competing financial interests or personal relationships that could have appeared to influence the work reported in this paper.

Acknowledgement

This research was conducted within the framework of the VALOstones project (Grant Agreement No. 1837), funded by National Funding Agencies from France (French National Research Agency – ANR), Tunisia (Ministry of Higher Education and Scientific Research – MHESR), Italy (Ministry of Universities and Research – MUR), Türkiye (Scientific and Technological Research Council of Türkiye – TÜBITAK), and Morocco (Ministry of Higher Education, Scientific Research and Innovation – MESRSI). The project is supported under the Partnership for Research and Innovation in the Mediterranean Area (PRIMA), and co-funded by the European Union's Horizon 2020 Framework Programme for Research and Innovation.

Appendix A. Supplementary data

Supplementary data to this article can be found online at https://doi.org/10.1016/j.foodchem.2025.147134.

Data availability

Data will be made available on request.

References

Anukam, A., & Berghel, J. (2020). Biomass pretreatment and characterization: A review. *In Biotechnological Applications of Biomass*. https://doi.org/10.5772/intechopen.93607

Bai, Y., Arulrajah, A., Horpibulsuk, S., & Chu, J. (2023). Gasified olive stone biochar as a green construction fill material. *Construction and Building Materials, 403*, Article 133003. https://doi.org/10.1016/j.conbuildmat.2023.133003

Baranyi, J., & Roberts, T. A. (1994). A dynamic approach to predicting bacterial growth in food. *International Journal of Food Microbiology, 23*, 277–294. https://doi.org/10.1016/0168-1605(94)90157-0

Bartolomei, M., Bollati, C., Bellumori, M., Cecchi, L., Cruz-Chamorro, I., Santos-Sánchez, G., Ranaldi, G., Ferruzza, S., Sambuy, Y., Arnoldi, A., Mulinacci, N., &

Lammi, C. (2021). Extra virgin olive oil phenolic extract on human hepatic HepG2 and intestinal Caco-2 cells: Assessment of the antioxidant activity and intestinal trans-epithelial transport. *Antioxidants, 10*(1), 1–20. https://doi.org/10.3390/antiox10010118

Bazzaz, B. S. F., Khameneh, B., Ostad, M. R. Z., & Hosseinzadeh, H. (2018). *In vitro* evaluation of antibacterial activity of verbascoside, lemon verbena extract and caffeine in combination with gentamicin against drug-resistant *Staphylococcus aureus* and *Escherichia coli* clinical isolates. *Avicenna Journal of Phytomedicine, 8*(3), 246–253.

Benzie, I. F. F., & Strain, J. J. (1996). The ferric reducing ability of plasma (FRAP) as a measure of "antioxidant power": The FRAP assay. *Analytical Biochemistry, 239*(1), 70–76. https://doi.org/10.1006/abio.1996.0292

Berbel, J., & Posadillo, A. (2018). Review and analysis of alternatives for the valorisation of agro-industrial olive oil by-products. *Sustainability, 10*(1), 237. https://doi.org/10.3390/su10010237

Bisson, G., Maifreni, M., Innocente, N., & Marino, M. (2023). Application of pre-adaptation strategies to improve the growth of probiotic lactobacilli under food-relevant stressful conditions. *Food & Function, 14*(4), 2128–2137. https://doi.org/10.1039/d2fo03215e

Bolek, S. (2020). Olive stone powder: A potential source of fiber and antioxidant and its effect on the rheological characteristics of biscuit dough and quality. *Innovative Food Science & Emerging Technologies, 64*, Article 102423. https://doi.org/10.1016/j.ifset.2020.102423

Brand-Williams, W., Cuvelier, M. E., & Berset, C. (1995). Use of a free radical method to evaluate antioxidant activity. *LWT, 28*(1), 25–30. https://doi.org/10.1016/s0023-6438(95)80008-5

Cakir, E., Yildirim, R. M., Pour, N. K., Ozulku, G., Toker, O. S., & Arici, M. (2023). Possibility of using black olive seed powder in formulations to functionalize bread. *Latin American Applied Research, 53*(4), 395–401. https://doi.org/10.52292/j.laar.2023.1073

Carraro, L., Trocino, A., & Xiccato, G. (2005). Dietary supplementation with olive stone meal in growing rabbits. *Italian Journal of Animal Science, 4*(3), 88–90. https://doi.org/10.4081/ijas.2005.3s.88

Chen, J., Ma, X., Liang, M., Guo, Z., Cai, Y., Zhu, C., … Ying, H. (2024). Physical–chemical–biological pretreatment for biomass degradation and industrial applications: A review. *Waste, 2*(4), 451–473. https://doi.org/10.3390/WASTE2040024

Cheok, C. Y., Chin, N. L., Yusof, Y. A., Talib, R. A., & Law, C. L. (2013). Optimization of total monomeric anthocyanin (TMA) and total phenolic content (TPC) extractions from mangosteen (*Garcinia mangostana Linn.*) hull using ultrasonic treatments. *Industrial Crops and Products, 50*, 1–7. https://doi.org/10.1016/j.indcrop.2013.07.024

Christoforou, E., & Fokaides, P. A. (2016). A review of olive mill solid wastes to energy utilization techniques. *Waste Management, 49*, 346–363. https://doi.org/10.1016/j.wasman.2016.01.012

Cuevas, M., García Martín, J. F., Bravo, V., & Sánchez, S. (2021). Ethanol production from olive stones through liquid hot water pre-treatment, enzymatic hydrolysis and fermentation. *Fermentation, 7*(1). https://doi.org/10.3390/fermentation7010025

Daglia, M. (2012). Polyphenols as antimicrobial agents. *Current Opinion in Biotechnology, 23*(2), 174–181. https://doi.org/10.1016/j.copbio.2011.08.007

Deng, W., Hu, J., Rong, M., Zhang, C., Wen, H., Liu, Y., … Hu, J. (2024). Ultrafine starch particles as Pickering emulsion stabilizers with different interfacial behaviors. *Starch - Stärke, 76*(9–10), Article 2400028. https://doi.org/10.1002/star.202400028

Di Mattia, C. D., Sacchetti, G., Mastrocola, D., Sarker, D. K., & Pittia, P. (2010). Surface properties of phenolic compounds and their influence on the dispersion degree and oxidative stability of olive oil O/W emulsions. *Food Hydrocolloids, 24*(6–7), 652–658. https://doi.org/10.1016/j.foodhyd.2010.03.007

Doménech, P., Duque, A., Higueras, I., Fernández, J. L., & Manzanares, P. (2021). Analytical characterization of water-soluble constituents in olive-derived by-products. *Foods, 10*(6), 1299. https://doi.org/10.3390/foods10061299

Donner, M., Erraach, Y., López-i-Gelats, F., Manuel-i-Martin, J., Yatribi, T., Radić, I., & El Hadad-Gauthier, F. (2022). Circular bioeconomy for olive oil waste and by-product valorisation: Actors' strategies and conditions in the Mediterranean area. *Journal of Environmental Management, 321*, Article 115836. https://doi.org/10.1016/j.jenvman.2022.115836

Enaime, G., Dababat, S., Wichern, M., & Lübken, M. (2024). Olive mill wastes: From wastes to resources. *Environmental Science and Pollution Research, 31*(14), 20853–20880. https://doi.org/10.1007/s11356-024-32468-x

Faraji, H., & Lindsay, R. C. (2004). Characterisation of the antioxidant activity of sugars and polyhydric alcohols in fish oil emulsions. *Journal of Agricultural and Food Chemistry, 52*(23), 7164–7171. https://doi.org/10.1021/jf035291k

Feng, Z., Li, L., Zhang, Y., Li, X., Liu, C., Jiang, B., Xu, J., & Sun, Z. (2019). Formation of whey protein isolate nanofibrils by endoproteinase GluC and their emulsifying properties. *Food Hydrocolloids, 94*, 71–79. https://doi.org/10.1016/j.foodhyd.2019.03.004

Ferreiro-Cabello, J., Fraile-Garcia, E., Pernia-Espinoza, A., & Martinez-de-Pison, F. J. (2022). Strength performance of different mortars doped using olive stones as lightweight aggregate. *Buildings, 12*(10), 1668. https://doi.org/10.3390/buildings12101668

Freitas, P. A. V., González-Martínez, C., & Chiralt, A. (2022). Applying ultrasound-assisted processing to obtain cellulose fibres from rice straw to be used as reinforcing agents. *Innovative Food Science & Emerging Technologies, 76*, Article 102932. https://doi.org/10.1016/J.IFSET.2022.102932

Gomes-Araújo, R., Martínez-Vázquez, D. G., Charles-Rodríguez, A. V., Rangel-Ortega, S., & Robledo-Olivo, A. (2021). Bioactive compounds from agricultural residues, their obtaining techniques, and the antimicrobial effect as postharvest additives. *International Journal of Food Science, 2021*, Article 9936722. https://doi.org/10.1155/2021/9936722

Gómez-Cruz, I., Contreras, M. D. M., Carvalheiro, F., Duarte, L. C., Roseiro, L. B., Romero, I., & Castro, E. (2021). Recovery of bioactive compounds from industrial exhausted olive pomace through ultrasound-assisted extraction. *Biology, 10*(6), 514. https://doi.org/10.3390/biology10060514

Gomez-Martin, A., Chacartegui, R., Ramirez-Rico, J., & Martinez-Fernandez, J. (2018). Performance improvement in olive stone's combustion from a previous carbonization transformation. *Fuel, 228*, 254–262. https://doi.org/10.1016/j.fuel.2018.04.127

Gullón, B., Gullón, P., Eibes, G., Cara, C., De Torres, A., López-Linares, J. C., … Castro, E. (2018). Valorisation of olive agro-industrial by-products as a source of bioactive compounds. *Science of the Total Environment, 645*, 533–542. https://doi.org/10.1016/j.scitotenv.2018.07.155

Hromádková, Z., Ebringerová, A., & Valachovič, P. (1999). Comparison of classical and ultrasound-assisted extraction of polysaccharides from *Salvia officinalis L. Ultrasonics Sonochemistry, 5*(4), 163–168. https://doi.org/10.1016/s1350-4177(98)00046-7

Innocente, N., Marino, M., & Calligaris, S. (2019). Recovery of brines from cheesemaking using high-pressure homogenization treatments. *Journal of Food Engineering, 247*, 188–194. https://doi.org/10.1016/j.jfoodeng.2018.12.012

IOC. (2022). *The world of olive oil.* International Olive Council.

Irakli, M., Chatzopoulou, P., & Ekateriniadou, L. (2018). Optimization of ultrasound-assisted extraction of phenolic compounds: Oleuropein, phenolic acids, phenolic alcohols and flavonoids from olive leaves and evaluation of its antioxidant activities. *Industrial Crops and Products, 124*, 382–388. https://doi.org/10.1016/j.indcrop.2018.07.070

Jahanbakhshi, R., & Ansari, S. (2020). Physicochemical properties of sponge cake fortified by olive stone powder. *Journal of Food Quality, 2020*(1), Article 1493638. https://doi.org/10.1155/2020/1493638

Jambrak, A. R., Herceg, Z., Šubarić, D., Babić, J., Brnčić, M., Brnčić, S. R., & Gelo, J. (2010). Ultrasound effect on physical properties of corn starch. *Carbohydrate Polymers, 79*(1), 91–100. https://doi.org/10.1016/j.carbpol.2009.07.051

Jambrak, A. R., Mason, T. J., Paniwnyk, L., & Lelas, V. (2007). Ultrasonic effect on pH, electric conductivity, and tissue surface of button mushrooms, Brussels sprouts and cauliflower. *Czech Journal of Food Sciences, 25*(2), 90–100.

Juttuporn, W., Thiengkaew, P., Rodklongtan, A., Rodprapakorn, M., & Chitprasert, P. (2018). Ultrasound-assisted extraction of antioxidant and antibacterial phenolic compounds from steam-exploded sugarcane bagasse. *Sugar Tech, 20*(5), 599–608. https://doi.org/10.1007/s12355-017-0582-y

Kaur, H., & Gill, B. S. (2019). Effect of high-intensity ultrasound treatment on nutritional, rheological and structural properties of starches obtained from different cereals. *International Journal of Biological Macromolecules, 126*, 367–375. https://doi.org/10.1016/j.ijbiomac.2018.12.149

Kim, Y. K., Roy, P. K., Ashrafudoulla, M., Nahar, S., Toushik, S. H., Hossain, M. I., … Ha, S. D. (2022). Antibiofilm effects of quercetin against *Salmonella enterica* biofilm formation and virulence, stress response, and quorum-sensing gene expression. *Food Control, 137*, Article 108964. https://doi.org/10.1016/j.foodcont.2022.108964

de Koster, C. G., & Brul, S. (2016). MALDI-TOF MS identification and tracking of food spoilers and food-borne pathogens. *Current Opinion in Food Science, 10*, 76–84. https://doi.org/10.1016/j.cofs.2016.11.004

Kumar, G., Le, D. T., Durco, J., Cianciosi, S., Devkota, L., & Dhital, S. (2023). Innovations in legume processing: Ultrasound-based strategies for enhanced legume hydration and processing. *Trends in Food Science & Technology, 139*, Article 104122. https://doi.org/10.1016/j.tifs.2023.104122

Lima, V. N., Oliveira-Tintino, C. D. M., Santos, E. S., Morais, L. P., Tintino, S. R., Freitas, T. S., … Coutinho, H. D. M. (2016). Antimicrobial and enhancement of the antibiotic activity by phenolic compounds: Gallic acid, caffeic acid and pyrogallol. *Microbial Pathogenesis, 99*, 56–61. https://doi.org/10.1016/j.micpath.2016.08.004

Lo Bianco, R., Losciale, P., Manfrini, L., & Corelli Grappadelli, L. (2015). Possible role of mannitol as an oxygen radical scavenger in olive. *Acta Horticulturae, 924*, 83–88. https://iris.unipa.it/handle/10447/65834.

Maalej, A., Forte, M., Bouallagui, Z., Donato, S., Mita, L., Mita, D. G., & Sayadi, S. (2017). Olive compounds attenuate oxidative damage induced in HEK-293 cells via MAPK signaling pathway. *Journal of Functional Foods, 39*, 18–27. https://doi.org/10.1016/j.jff.2017.10.008

Mallamaci, R., Budriesi, R., Clodoveo, M. L., Biotti, G., Micucci, M., Ragusa, A., … Franchini, C. (2021). Olive tree in circular economy as a source of secondary metabolites active for human and animal health beyond oxidative stress and inflammation. *Molecules, 26*(4), 1072. https://doi.org/10.3390/molecules26041072

Manzanares, P., Ballesteros, I., Negro, M. J., González, A., Oliva, J. M., & Ballesteros, M. (2020). Processing of extracted olive oil pomace residue by hydrothermal or dilute acid pretreatment and enzymatic hydrolysis in a biorefinery context. *Renewable Energy, 145*, 1235–1245. https://doi.org/10.1016/j.renene.2019.06.120

Martínez-Patiño, J. C., Gómez-Cruz, I., Romero, I., Gullón, B., Ruiz, E., Brnčić, M., & Castro, E. (2019). Ultrasound-assisted extraction as a first step in a biorefinery strategy for valorisation of extracted olive pomace. *Energies, 12*(14), 2679. https://doi.org/10.3390/en12142679

Martinez-Solano, K. C., Garcia-Carrera, N. A., Tejada-Ortigoza, V., García-Cayuela, T., & Garcia-Amezquita, L. E. (2021). Ultrasound application for the extraction and modification of fiber-rich by-products. *Food Engineering Reviews, 13*(3), 524–543. https://doi.org/10.1007/s12393-020-09269-2

Melchior, S., Codrich, M., Gorassini, A., Mehn, D., Ponti, J., Verardo, G., & Calligaris, S. (2023). Design and advanced characterization of quercetin-loaded nano-liposomes prepared by high-pressure homogenization. *Food Chemistry, 428*, Article 136680. https://doi.org/10.1016/j.foodchem.2023.136680

Melchior, S., Moretton, M., Calligaris, S., Manzocco, L., & Nicoli, M. C. (2022). High pressure homogenization shapes the techno-functionalities and digestibility of pea proteins. *Food and Bioproducts Processing, 131*, 77–85. https://doi.org/10.1016/j.fbp.2021.10.011

Mikkonen, K. S. (2020). Strategies for structuring diverse emulsion systems by using wood lignocellulose-derived stabilizers. *Green Chemistry, 22*(4), 1019–1037. https://doi.org/10.1039/C9GC04457D

Montegiove, N., Gambelli, A. M., Calzoni, E., Bertoldi, A., Puglia, D., Zadra, C., … Gigliotti, G. (2024). Biogas production with residuals deriving from olive mill wastewater and olive pomace wastes: Quantification of produced energy, spent energy, and process efficiency. *Agronomy, 14*(3), 531. https://doi.org/10.3390/agronomy14030531

Mujtaba, M., Fernandes Fraceto, L., Fazeli, M., Mukherjee, S., Savassa, S. M., Araujo de Medeiros, G., … Vilaplana, F. (2023). Lignocellulosic biomass from agricultural waste to the circular economy: A review with focus on biofuels, biocomposites and bioplastics. *Journal of Cleaner Production, 402*, Article 136815. https://doi.org/10.1016/J.JCLEPRO.2023.136815

Mumtaz, S., Mumtaz, S., Ali, S., Tahir, H. M., Kazmi, S. A. R., Mughal, T. A., & Younas, M. (2021). Evaluation of antibacterial activity of vitamin C against human bacterial pathogens. *Brazilian Journal of Biology, 83*, Article e247165. https://doi.org/10.1590/1519-6984.247165

Nair, R. B., Kalif, M., Ferreira, J. A., Taherzadeh, M. J., & Lennartsson, P. R. (2017). Mild-temperature dilute acid pretreatment for integration of first and second generation ethanol processes. *Bioresource Technology, 245*, 145–151. https://doi.org/10.1016/j.biortech.2017.08.125

Noparat, P., Prasertsan, P., Othong, S., & Pan, X. (2015). Dilute acid pretreatment of oil palm trunk biomass at high temperature for enzymatic hydrolysis. *Energy Procedia, 79*, 924–929. https://doi.org/10.1016/j.egypro.2015.11.588

Nunes, M. A., Pimentel, F. B., Costa, A. S. G., Alves, R. C., & Oliveira, M. B. P. P. (2016). Olive by-products for functional and food applications: Challenging opportunities to face environmental constraints. *Innovative Food Science & Emerging Technologies, 35*, 139–148. https://doi.org/10.1016/j.ifset.2016.04.016

Oncel, B., & Ozbek, C. (2025). Optimization of olive stone powder tea production: Infusion conditions, bioactive compounds, and sensory evaluation using response surface method. *Journal of Food Measurement and Characterization, 19*(6), 4278–4291. https://doi.org/10.1007/s11694-025-03252-3

Pace, L. R., Harrison, Z. L., Brown, M. N., Haggard, W. O., & Jennings, J. A. (2019). Characterization and antibiofilm activity of mannitol–chitosan-blended paste for local antibiotic delivery system. *Marine Drugs, 17*(9), 517. https://doi.org/10.3390/md17090517

Peng, F., Ren, J. L., Xu, F., Bian, J., Peng, P., & Sun, R. C. (2009). Comparative study of hemicelluloses obtained by graded ethanol precipitation from sugarcane bagasse. *Journal of Agricultural and Food Chemistry, 57*(14), 6305–6317. https://doi.org/10.1021/jf900986b

Rodríguez, G., Lama, A., Rodríguez, R., Jiménez, A., Guillén, R., & Fernández-Bolaños, J. (2008). Olive stone: An attractive source of bioactive and valuable compounds. *Bioresource Technology, 99*(13), 5261–5269. https://doi.org/10.1016/j.biortech.2007.11.027

Rodríguez, Ó., Bona, S., Stäbler, A., & Rodríguez-Turienzo, L. (2022). Ultrasound-assisted extraction of polyphenols from olive pomace: Scale up from laboratory to pilot scenario. *Processes, 10*(12), 2481. https://doi.org/10.3390/pr10122481

Saleh, M., Cuevas, M., García, J. F., & Sánchez, S. (2014). Valorization of olive stones for xylitol and ethanol production from dilute acid pretreatment via enzymatic hydrolysis and fermentation by *Pachysolen tannophilus*. *Biochemical Engineering Journal, 90*, 286–293. https://doi.org/10.1016/j.bej.2014.06.023

Sánchez-Borrego, F. J., Barea de Hoyos-Limón, T. J., García-Martín, J. F., & Álvarez-Mateos, P. (2021). Production of bio-oils and biochars from olive stones: Application of biochars to the esterification of oleic acid. *Plants, 11*(1), 70. https://doi.org/10.3390/plants11010070

Serafin, J., Dziejarski, B., & Sreńscek-Nazzal, J. (2023). An innovative and environmentally friendly bioorganic synthesis of activated carbon based on olive stones and its potential application for CO_2 capture. *Sustainable Materials and Technologies, 38*, Article e00717. https://doi.org/10.1016/j.susmat.2023.e00717

Setyaningsih, W., Hidayah, N., Saputro, I. E., Palma, M., & García Barroso, C. (2016). Profile of phenolic compounds in Indonesian rice (*Oryza sativa*) varieties throughout post-harvest practices. *Journal of Food Composition and Analysis, 54*, 55–62. https://doi.org/10.1016/j.jfca.2016.10.004

Sidana, A., & Yadav, S. K. (2022). Recent developments in lignocellulosic biomass pretreatment with a focus on eco-friendly, non-conventional methods. *Journal of Cleaner Production, 335*, Article 130286. https://doi.org/10.1016/j.jclepro.2021.130286

Singleton, V. L., & Rossi, J. A. (1965). Colorimetry of total phenolics with phosphomolybdic-phosphotungstic acid reagents. *American Journal of Enology and Viticulture, 16*(3), 144–158. https://doi.org/10.5344/ajev.1965.16.3.144

Siracusa, G., La Rosa, A. D., Siracusa, V., & Trovato, M. (2001). Eco-compatible use of olive husk as filler in thermoplastic composites. *Journal of Polymers and the Environment, 9*(4), 157–161. https://doi.org/10.1023/A:1020465305193

Tian, L., Kejing, Y., Zhang, S., Yi, J., Zhu, Z., Decker, E. A., & McClements, D. J. (2021). Impact of tea polyphenols on the stability of oil-in-water emulsions coated by whey proteins. *Food Chemistry, 343*, Article 128448. https://doi.org/10.1016/j.foodchem.2020.128448

Valoppi, F., Lahtinen, M. H., Bhattarai, M., Kirjoranta, S. J., Juntti, V. K., Peltonen, L. J., … Mikkonen, K. S. (2019). Centrifugal fractionation of softwood extracts improves the biorefinery workflow and yields functional emulsifiers. *Green Chemistry, 21*(17), 4691–4705. https://doi.org/10.1039/C9GC02007A

Valoppi, F., Maina, N., Allén, M., Miglioli, R., Kilpeläinen, P. O., & Mikkonen, K. S. (2019). Spruce galactoglucomannan-stabilized emulsions as essential fatty acid delivery systems for functionalized drinkable yogurt and oat-based beverage. *European Food Research and Technology, 245*(7), 1387–1398. https://doi.org/10.1007/s00217-019-03273-5

Wang, C., Tallian, C., Su, J., Vielnascher, R., Silva, C., Cavaco-Paulo, A., … Fu, J. (2018). Ultrasound-assisted extraction of hemicellulose and phenolic compounds from bamboo bast fiber powder. *PLoS One, 13*(6), Article e0197537. https://doi.org/10.1371/journal.pone.0197537

Wang, S., Yao, J., Zhou, B., Yang, J., Chaudry, M. T., Wang, M., & Yin, W. (2018). Bacteriostatic effect of quercetin as an antibiotic alternative in vivo and its antibacterial mechanism *in vitro*. *Journal of Food Protection, 81*(1), 68–78. https://doi.org/10.4315/0362-028X.JFP-17-214

Wu, J., Chen, R., Tan, L., Bai, H., Tian, L., Lu, J., Gao, M., Bai, C., Sun, H., & Chi, Y. (2022). Ultrasonic disruption effects on the extraction efficiency, characterization, and bioactivities of polysaccharides from *Panax notoginseng* flower. *Carbohydrate Polymers, 291*, Article 119535. https://doi.org/10.1016/j.carbpol.2022.119535

Xie, H., Wei, X., Liu, X., Bai, W., & Zeng, X. (2023). Effect of polyphenolic structure and mass ratio on the emulsifying performance and stability of emulsions stabilized by polyphenol-corn amylose complexes. *Ultrasonics Sonochemistry, 95*, Article 106367. https://doi.org/10.1016/j.ultsonch.2023.106367

Yang, W., Ajapur, V. K., Krishnamurthy, K., Feng, H., Yang, R., & Rababah, T. M. (2009). Expedited extraction of xylan from corncob by power ultrasound. *International Journal of Agricultural and Biological Engineering, 2*(4), 76–83. https://doi.org/10.3965/j.issn.1934-6344.2009.04.076-083